Long-Timescale Molecular Dynamics Simulations Elucidate the Dynamics and Kinetics of Exposure of the Hydrophobic Patch in Troponin C

Steffen Lindert,[†‡*] Peter M. Kekenes-Huskey,[†‡] and J. Andrew McCammon[†‡§¶]

[†]Department of Pharmacology, University of California San Diego, La Jolla, California; [‡]National Science Foundation Center for Theoretical Biological Physics, La Jolla, California; [§]Howard Hughes Medical Institute, University of California San Diego, La Jolla, California; and [¶]Department of Chemistry and Biochemistry, National Biomedical Computation Resource, University of California San Diego, La Jolla, California

ABSTRACT Troponin (Tn) is an important regulatory protein in the thin-filament complex of cardiomyocytes. Calcium binding to the troponin C (TnC) subunit causes a change in its dynamics that leads to the transient opening of a hydrophobic patch on TnC's surface, to which a helix of another subunit, troponin I (TnI), binds. This process initiates contraction, making it an important target for studies investigating the detailed molecular processes that underlie contraction. Here we use microsecond-timescale Anton molecular dynamics simulations to investigate the dynamics and kinetics of the opening transition of the TnC hydrophobic patch. Free-energy differences for opening are calculated for wild-type Ca^{2+}-bound TnC (~8 kcal/mol), V44Q Ca^{2+}-bound TnC (3.2 kcal/mol), E40A Ca^{2+}-bound TnC (~12 kcal/mol), and wild-type apo TnC (~20 kcal/mol). These results suggest that the mutations have a profound impact on the frequency with which the hydrophobic patch presents to TnI. In addition, these simulations corroborate that cardiac wild-type TnC does not open on timescales relevant to contraction without calcium being bound.

INTRODUCTION

Cardiac troponin (Tn) is an important regulatory protein complex in the thin-filament complex of the sarcomere in cardiomyocytes. It initiates a chain of events that allow the cell to contract, a process that is of paramount importance to proper heart function. Tn consists of three subunits: troponin C (TnC), troponin I (TnI), and troponin T (TnT) (1). When the signaling ion, Ca^{2+}, binds to the terminal regulatory domain of TnC, structural and dynamic changes result that initiate sarcomere contraction (2). A significant effect of calcium binding to the regulatory domain of TnC is the exposure of a hydrophobic patch on TnC's surface. The switch region of Troponin I (TnI) subsequently associates with this hydrophobic patch, loosening the inhibition of TnI on tropomyosin and actin. This process culminates in the release of TnI's inhibition of myosin binding, and contraction ensues (2,3). Although Ca^{2+}-binding to the 89-residue terminal regulatory domain of TnC has been studied in detail before (4–6), this work focuses on TnC dynamics exposing the hydrophobic patch. Computationally elucidating these events marks one additional step toward understanding, on a molecular basis, the cellular processes governing contraction.

NMR and x-ray crystallography have shed ample light on the structure of the TnC regulatory domain (7–10). The regulatory domain, a highly α-helical molecule that constitutes the first 89 terminal residues of the troponin C protein, consists of five α-helices (N, A–D). Helices A–D comprise two EF-hand helix-loop-helix motifs. The EF hands, which are known to be metal-binding sites, are labeled I and II (11). Site II, the low-affinity, Ca^{2+}-specific Ca^{2+}-binding site is generally considered the only site directly involved in calcium regulation of cardiac muscle contraction (12). Ca^{2+}-binding to site II of cardiac TnC does not induce an opening transition akin to skeletal TnC (13) but leaves the structure more or less unperturbed in the closed conformation (7,14). It is believed that the TnI switch peptide has to be present to stabilize the open conformation of the Ca^{2+}-bound regulatory domain of cardiac TnC (8,15) suggesting that the open conformation may only be a transient state that is sampled by TnC after Ca^{2+} binding (6). Structures of the apo state, the Ca^{2+}-bound state, and the Ca^{2+}-TnI-switch-peptide-bound state have been determined, giving valuable snapshots of the closed and open conformations, respectively, of the TnC hydrophobic patch. In addition to the structural properties of TnC, the kinetics of its association have been investigated experimentally, at least for skeletal muscle (16).

An aspect that has not yet been extensively studied computationally is the association of the TnI switch peptide with TnC and the dynamical processes in TnC that support this association. Atomistic-level computational studies of TnC in various states of calcium and TnI switch peptide association are necessary to investigate these phenomena. Assuming that the frequency of opening is in the high-nanosecond or low-microsecond regime, long-timescale simulations may even have the potential to quantitatively investigate the kinetics of opening and closing of the TnC hydrophobic

Submitted July 16, 2012, and accepted for publication August 20, 2012.

*Correspondence: slindert@ucsd.edu

Editor: Nathan Baker.

0006-3495/12/10/1784/6 $2.00

http://dx.doi.org/10.1016/j.bpj.2012.08.058

patch. In this study, we used the Anton supercomputer (17) to perform microsecond-timescale molecular dynamics (MD) simulations of TnC in its apo and Ca^{2+}-bound states. Long-timescale simulations of Ca^{2+}-bound TnC gain-of-function mutant V44Q (18,19) and loss-of-function mutant E40A (18) were also carried out. Kinetics and a free-energy difference of the opening-closing process are extracted from the simulations. The results of these studies give a quantitative appreciation of the processes involved in TnI binding to TnC and may be able to guide the improvement of inotropic pharmaceuticals that target TnC.

MATERIALS AND METHODS

System preparation

Four different systems of the terminal regulatory domain of human cardiac troponin C (wild-type apo TnC, wild-type Ca^{2+}-bound TnC, V44Q Ca^{2+}-bound TnC, and E40A Ca^{2+}-bound TnC) were run on Anton. The initial preparation of the systems was described in (P.M. Kekenes-Huskey, S. Lindert, and J.A. McCammon, unpublished, and (6)). Well-equilibrated structures after at least 100 ns of MD were used as input for the Anton system preparation. According to the instructions on the Anton wiki, the scripts amber_topNrst2cms.py, convertNAMDtoMaestro.2.5.py, viparr.py, and build_constraints.py were used to generate cms system files. The script mae2dms converted the cms files into dms format. Subsequently, guess_chem, refinesigma, and subboxer were used to prepare all the input files for the actual simulation. All simulated systems contained explicit solvent.

Anton MD simulations

All Anton simulations were performed under the NPT ensemble at 300 K using a Berendsen thermostat and barostat. Bonds involving hydrogen atoms were constrained using the SHAKE algorithm (20), allowing for a time step of 2 fs. Structures were saved every 100.002 ps. Production runs were carried out on the 512-node Anton machine, running 15 jobsteps for the wild-type apo TnC, 49 jobsteps for the wild-type Ca^{2+}-bound TnC, 34 jobsteps for the V44Q Ca^{2+}-bound TnC, and 15 jobsteps for the E40A Ca^{2+}-bound TnC. A jobstep is an Anton-specific unit of simulation time. It corresponds to running on all 512 nodes for a time period of 30 min. This corresponds to a total simulation time of 1.16 μs for the wild-type apo TnC, 9.75 μs for the wild-type Ca^{2+}-bound TnC, 3.96 μs for the V44Q Ca^{2+}-bound TnC, and 1.79 μs for the E40A Ca^{2+}-bound TnC.

Interhelical-angle analysis and estimation of free-energy cost of opening the hydrophobic patch

The degree of opening of the hydrophobic patch can best be described by the interhelical angle between helices A and B (21). For the analysis of interhelical angles, angles were calculated using interhlx (K. Yap, University of Toronto, Ontario, Canada). Using interhelical-angle analysis, the degree of openness for every frame of the trajectory can be determined. Defining a cutoff angle below which a state will be characterized as open and above which a state will be characterized as closed, the Boltzmann distribution of states is used to derive the free-energy difference ΔG from the occupancies of the open and closed states. $\Delta G = kT \ln N_{closed}/N_{open}$, where k is the Boltzmann constant, T is the temperature of the system, and N_{closed} and N_{open} are the number of systems found in the closed and open states, respectively, during the simulation. An A/B interhelical angle of 90° will be considered the most accurate criterion for defining a structure to be open, since all experimentally determined TnI-bound structures of TnC exhibit interhelical angles of ~90°. For the analysis, several different cutoff angles were used. Assuming that, for example, structures with interhelical angles below equally spaced values between 90° and 130° are considered open, free-energy differences for the system transitioning into these semiopen conformations can be computed. For example, using a 105° cutoff angle for the wild-type Ca^{2+}-bound TnC simulation, 14 frames (N_{open}) in this semiopen conformation (below interhelical angle 105°) are counted, whereas 97,503 frames (N_{closed}) of the trajectory exhibit an interhelical angle >105°. According to the Boltzmann distribution, this translates into a free-energy difference between the closed and open states (defined by the 105° cutoff angle) of 5.25 kcal/mol. This procedure makes it possible to extrapolate the free energy even if the trajectory did not contain any opening event to 90°. We assume a linear extrapolation to be valid, since we see a linear ΔG-versus-cutoff angle behavior for the V44Q case and there is nothing obvious about the other structures that might prevent them from opening the entire way.

RESULTS AND DISCUSSION

Microsecond Anton simulations show full opening events for V44Q mutant and partial opening events for wild-type TnC

Binding of calcium to TnC initiates a chain of events that eventually lead to contraction of the heart muscle cell. The second step in the process after binding of calcium is the exposure of a hydrophobic patch between helices A and B. The TnI switch peptide then binds to the hydrophobic surface, in turn disrupting the inhibition interaction between TnI and tropomyosin on the actin filament. Opening of the hydrophobic patch is a rare event and thus has only been observed once before in an accelerated MD simulation (6). To gauge the timescale and kinetics of this rare event, microsecond simulations on wild-type Ca^{2+}-bound TnC, V44Q Ca^{2+}-bound TnC, E40A Ca^{2+}-bound TnC, and wild-type apo TnC were performed on Anton (17). The degree of opening of the hydrophobic patch can best be described by the interhelical angle between helices A and B (21). Fig. 1 shows the A/B interhelical angle as a function of simulation time for the wild-type Ca^{2+}-bound TnC, V44Q Ca^{2+}-bound TnC, E40A Ca^{2+}-bound TnC, and wild-type apo TnC simulations. All simulations except the V44Q mutation display an average interhelical angle of ~135°, in agreement with all experimentally determined calcium-bound cardiac TnC structures having interhelical A/B angles of ~135°. The effect of the V44Q mutation changes the dynamics of the molecule as fluctuations are observed about an average interhelical A/B angle of 110°. This conformation is still closed on average but is more predisposed to open. The simulations are converged in terms of the A/B interhelical angle. Sudden increases in interhelical angle that can be seen toward the end of the wild-type-Ca^{2+}-bound and wild-type-apo-TnC simulations are most likely transient shifts toward a higher interhelical angle such as the one observed in a previously published accelerated MD simulation of wild-type Ca^{2+}-bound TnC (6).

There are, however, strong differences between the systems when it comes to opening events. The Anton

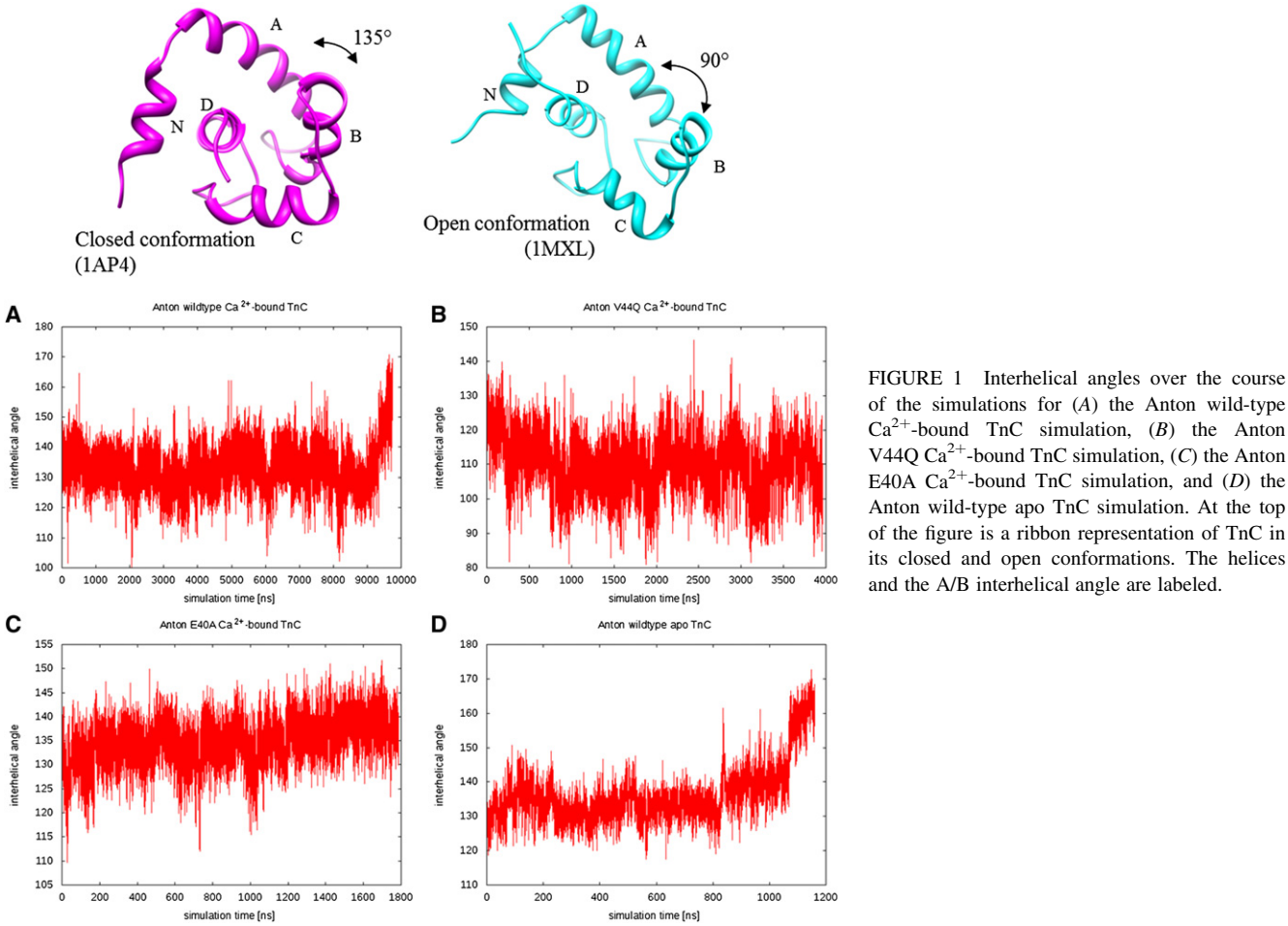

FIGURE 1 Interhelical angles over the course of the simulations for (*A*) the Anton wild-type Ca^{2+}-bound TnC simulation, (*B*) the Anton V44Q Ca^{2+}-bound TnC simulation, (*C*) the Anton E40A Ca^{2+}-bound TnC simulation, and (*D*) the Anton wild-type apo TnC simulation. At the top of the figure is a ribbon representation of TnC in its closed and open conformations. The helices and the A/B interhelical angle are labeled.

wild-type Ca^{2+}-bound trajectory opens 12 times below 105°, 76 times below 110°, and 291 times below 115° over the course of ~10 μs. The most open conformation observed in 10 μs of simulation has an A/B interhelical angle of 100.2°. The V44Q mutation, characterized as a gain-of-function mutation (18), causes a massive increase in opening events. The Anton V44Q Ca^{2+}-bound trajectory opens 15 times below 85°, 142 times below 90°, and 742 times below 95° over the course of ~4 μs. For comparison, there are 3652 opening events below 105° within just 4 μs in this trajectory. The most open A/B interhelical angle observed is 80.9°. For illustration purposes, Fig. 2 shows two configurations extracted from the Anton V44Q Ca^{2+}-bound trajectory. Fig. 2 *A* shows the protein in its closed conformation (interhelical A/B angle 135.1°) at the beginning of the trajectory. There is no noticeable cleft between helices A and B. Fig. 2 *B* depicts the protein in its open conformation (after ~1.9 μs of simulation time, interhelical A/B angle 80.9°), where a deep hydrophobic pocket has been formed by helix B moving away from helix A. The TnI switch peptide can bind to this pocket. In contrast, the E40A mutation, characterized as a loss-of-function mutation, has the opposite effect. The opening events seen here are less pronounced and less frequent. The Anton E40A Ca^{2+}-bound trajectory opens once below 110°, five times below 115°, and 61 times below 120° over the course of ~2 μs. The most open A/B interhelical angle observed in this simulation is 109.7°. The most closed conformations, however, are observed in the Anton wild-type apo trajectory, which opens only six times below 120° and 208 times below 125° over the course of ~1.2 μs. The most open A/B

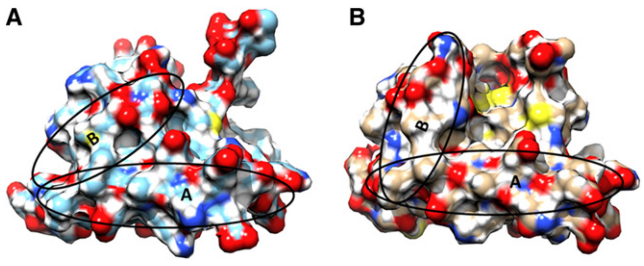

FIGURE 2 Surface representation of a closed and an open conformation from the Anton V44Q Ca^{2+}-bound TnC simulation. (*A*) TnC in its closed conformation at the beginning of the trajectory. The interhelical A/B angle is 135.1°. (*B*) TnC in its open conformation, after ~1.9 μs of simulation time. The interhelical A/B angle is 80.9°. Helices A and B are labeled for clarity.

interhelical angle observed in the apo simulation is 117.5°. These long-timescale findings corroborate results reported in (6) (and P.M. Kekenes-Huskey, S. Lindert, and J.A. McCammon, unpublished), in that there are virtually no opening events for an apo-TnC system. This is in agreement with calcium binding being necessary (but not sufficient) for TnI association to cardiac TnC (2). As speculated, more frequent and more pronounced opening events are seen in microsecond simulations of Ca^{2+}-bound TnC. The effects of the mutations seem to directly influence opening-closing dynamics, resulting in increased opening for the gain-of-function mutant and decreased opening for the loss-of-function mutant with respect to wild-type.

Free-energy difference for the opening transition estimated from simulations

In addition to a qualitative evaluation of the propensity of opening of the individual structures, the microsecond-timescale Anton simulations allow for a quantitative analysis of the process of opening the hydrophobic patch in TnC. The Boltzmann distribution of states was used to derive the free-energy difference, ΔG, based on the occupancies of the open and closed states, $\Delta G = kT \ln N_{\text{closed}}/N_{\text{open}}$. Although the experimentally determined TnI-bound structures of TnC all exhibit A/B interhelical angles of ~90° (which will be considered the most accurate criterion of defining a structure to be open), we used a more flexible criterion in the analysis. Assuming that, for example, structures with interhelical angles below equally spaced values between 90° and 130° are considered open, free-energy differences for the system transitioning into these semiopen conformations can be computed. Fig. 3 shows computed free-energy differences between open and closed states for multiple angles for the systems under investigation. There is a clear, linear relationship between the interhelical open/closed cutoff angle and the free-energy difference separating the open and closed states. The Anton V44Q Ca^{2+}-bound trajectory is the only simulation that allowed for direct observation of opening events below 90° within the low-microsecond simulation time. Therefore, a free-energy difference for opening of 3.2 kcal/mol can be directly extracted from the data. None of the other simulations opened up to a 90° interhelical angle. Using the linear relationship apparent in the data, however, it is possible to extrapolate the free energy of opening the hydrophobic patch to be ~8 kcal/mol for wild-type Ca^{2+}-bound TnC, ~12 kcal/mol for the E40A mutant of Ca^{2+}-bound TnC, and~20 kcal/mol for wild-type apo TnC. The time between opening events is another quantity that can be extracted from the simulations and is directly proportional to the free-energy difference. Fig. 4 shows the time between opening events for multiple open/closed angles for the simulated systems. Again, there seems to be a linear relationship between the angle and the logarithm of the average time between opening events. The V44Q TnC mutant opens to <90° on average every 28 ns, a value directly obtained from the simulation. For all other systems under investigation, extrapolation is used to determine the frequency of opening events. Wild-type Ca^{2+}-bound TnC opens every 50 μs to <90°; the E40A mutant of TnC opens every ~10 ms, whereas the extrapolated value for the wild-type apo TnC is well beyond the second regime. These simulations thus corroborate that cardiac wild-type TnC does not open on timescales relevant to contraction without calcium being bound. We are also able to predict that at least a millisecond of simulation time is necessary to observe a significant number of opening events in the wild-type Ca^{2+}-bound TnC system.

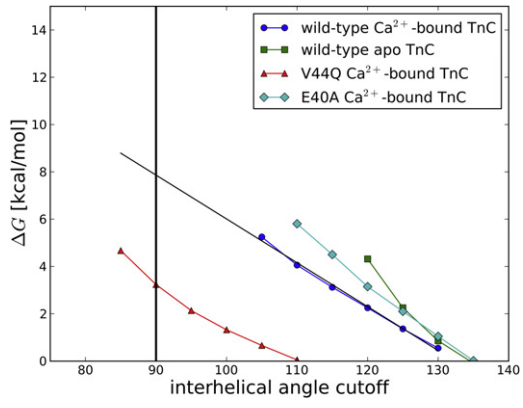

FIGURE 3 Dependence of computed free-energy differences between open and closed states on the cutoff angle. Values for the Anton wild-type Ca^{2+}-bound TnC simulation, the Anton V44Q Ca^{2+}-bound TnC simulation, the Anton E40A Ca^{2+}-bound TnC simulation, and the Anton wild-type apo TnC simulation are shown. Free energies are calculated based on the Boltzmann distribution of states. The widely accepted open-closed cutoff criterion of 90° is marked by a vertical black line.

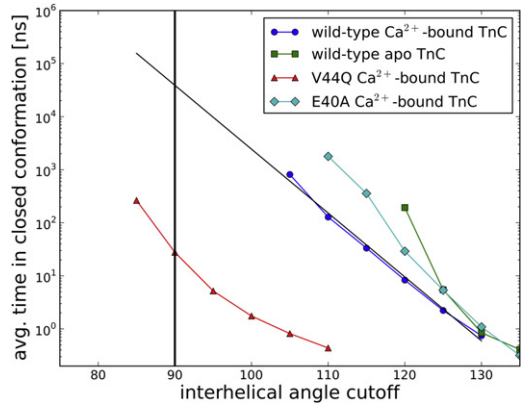

FIGURE 4 Dependence of average simulation time between opening events on the cutoff angle. Values for the Anton wild-type Ca^{2+}-bound TnC simulation, the Anton V44Q Ca^{2+}-bound TnC simulation, the Anton E40A Ca^{2+}-bound TnC simulation, and the Anton wild-type apo TnC simulation are shown. The widely accepted open-closed cutoff criterion of 90° is marked by a vertical black line.

CONCLUSION

Microsecond-timescale Anton simulations were used to investigate the exposure of the hydrophobic patch in Ca^{2+}-bound TnC and some of its mutants. Not only could the dynamics of a single exposure event be seen in the simulations; a sufficient number of opening events were observed to also extract the kinetics of opening. A free-energy estimate for the transition from the closed to open states was obtained for the different simulated systems. The free energy for opening increased from the V44Q mutant to the wild-type protein to the E40A mutant. The increased or decreased frequency of exposure of the hydrophobic patch, and thus increased or decreased opportunity for binding the TnI switch peptide, is consistent with V44Q being a gain-of-function mutation and E40A being a loss-of-function mutation. This, in addition to differences recently observed in calcium affinity (6) (and P.M. Kekenes-Huskey, S. Lindert, and J.A. McCammon, unpublished) establishes the modulated opening frequency of the hydrophobic patch as a leading factor by which the mutations control their different levels of function. A detailed discussion of the key changes in molecular interactions upon mutation can be found in (P.M. Kekenes-Huskey, S. Lindert, and J.A. McCammon, unpublished, and (6)) for both the V44Q and the E40A mutations. In summary, we speculate that the introduction of a polar residue into the hydrophobic patch (in the case of V44Q) destabilizes hydrophobic interactions, leading to an increase in opening frequency. In contrast, it is speculated that the replacement of a charged residue with an apolar amino acid in the hydrophobic patch (in the case of E40A) further stabilizes the hydrophobic interaction, resulting in a decrease in opening frequency. This is in agreement with reports by Tikunova and Davis (19), who speculated that introduction of a polar residue into the hydrophobic patch could lead the BC unit to move away from the NAD unit, in fact widening the opening angle.

To our knowledge, this is the most comprehensive computational investigation to date of the dynamics and kinetics of opening of the hydrophobic patch in TnC. Estimation of the free-energy cost for opening for different mutations is of great value to multiscale modeling approaches. The binding of the TnI switch peptide is one crucial input parameter for subcellular models of cardiomyocyte contractility. The ability to predict these parameters computationally offers great potential to complement experimental input by combining molecular and subcellular modeling techniques investigating myocyte contractility and the effect of mutations. In addition, the Anton simulations could be used in connection with relaxed-complex-scheme-type approaches (22) to find actionable pharmaceutical leads using structurally representative conformations for docking druglike small molecules. One possible therapeutic strategy may be to modulate TnI affinity to TnC by finding drugs that alter the dynamics of the opening or closing of the hydrophobic patch.

We thank Brian Sykes for interesting discussions concerning the opening transition of the hydrophobic patch. We also thank the members of the McCammon group for useful discussions.

This work was supported by the National Institutes of Health, the National Science Foundation, the Howard Hughes Medical Institute, the National Biomedical Computation Resource, and the National Science Foundation Supercomputer Centers. Computational resources were supported, in part, by National Science Foundation grant PHY-0822283, to the Center for Theoretical Biological Physics. S. L. was supported by the American Heart Association and the Center for Theoretical Biological Physics. Anton computer time was provided by the National Resource for Biomedical Supercomputing and the Pittsburgh Supercomputing Center through Grant NIH RC2GM093307 from the National Institutes of Health. The Anton machine had been donated generously by David E. Shaw; we are most grateful for the opportunity to use Anton. We thank Dr. Markus Dittrich and other staff at NRBSC for the support in using the Anton machine.

REFERENCES

1. Farah, C. S., and F. C. Reinach. 1995. The troponin complex and regulation of muscle contraction. *FASEB J.* 9:755–767.
2. Li, M. X., X. Wang, and B. D. Sykes. 2004. Structural based insights into the role of troponin in cardiac muscle pathophysiology. *J. Muscle Res. Cell Motil.* 25:559–579.
3. Kobayashi, T., and R. J. Solaro. 2005. Calcium, thin filaments, and the integrative biology of cardiac contractility. *Annu. Rev. Physiol.* 67:39–67.
4. Lim, C. C., H. Yang, …, R. Liao. 2008. A novel mutant cardiac troponin C disrupts molecular motions critical for calcium binding affinity and cardiomyocyte contractility. *Biophys. J.* 94:3577–3589.
5. Wang, D., I. M. Robertson, …, M. Regnier. 2012. Structural and functional consequences of the cardiac troponin C L48Q Ca^{2+}-sensitizing mutation. *Biochemistry.* In press.
6. Lindert, S., P. M. Kekenes-Huskey, …, J. A. McCammon. 2012. Dynamics and calcium association to the N-terminal regulatory domain of human cardiac troponin C: a multiscale computational study. *J. Phys. Chem. B.* 116:8449–8459.
7. Spyracopoulos, L., M. X. Li, …, B. D. Sykes. 1997. Calcium-induced structural transition in the regulatory domain of human cardiac troponin C. *Biochemistry.* 36:12138–12146.
8. Li, M. X., L. Spyracopoulos, and B. D. Sykes. 1999. Binding of cardiac troponin-I147-163 induces a structural opening in human cardiac troponin-C. *Biochemistry.* 38:8289–8298.
9. Robertson, I. M., Y. B. Sun, …, B. D. Sykes. 2010. A structural and functional perspective into the mechanism of Ca^{2+}-sensitizers that target the cardiac troponin complex. *J. Mol. Cell. Cardiol.* 49:1031–1041.
10. Gagné, S. M., M. X. Li, …, B. D. Sykes. 1998. The NMR angle on troponin C. *Biochem. Cell Biol.* 76:302–312.
11. Tobacman, L. S. 1996. Thin filament-mediated regulation of cardiac contraction. *Annu. Rev. Physiol.* 58:447–481.
12. Kobayashi, T., L. Jin, and P. P. de Tombe. 2008. Cardiac thin filament regulation. *Pflugers Arch.* 457:37–46.
13. Gagné, S. M., S. Tsuda, …, B. D. Sykes. 1995. Structures of the troponin C regulatory domains in the apo and calcium-saturated states. *Nat. Struct. Biol.* 2:784–789.
14. Sia, S. K., M. X. Li, …, B. D. Sykes. 1997. Structure of cardiac muscle troponin C unexpectedly reveals a closed regulatory domain. *J. Biol. Chem.* 272:18216–18221.
15. Dong, W. J., J. Xing, …, H. C. Cheung. 1999. Conformation of the regulatory domain of cardiac muscle troponin C in its complex with cardiac troponin I. *J. Biol. Chem.* 274:31382–31390.
16. Tripet, B., G. De Crescenzo, …, R. S. Hodges. 2002. Kinetic analysis of the interactions between troponin C and the C-terminal troponin I

regulatory region and validation of a new peptide delivery/capture system used for surface plasmon resonance. *J. Mol. Biol.* 323:345–362.

17. Shaw, D. E., M. M. Deneroff, …, S. C. Wang. 2008. Anton, a special-purpose machine for molecular dynamics simulation. *Commun. ACM.* 51:91–97.

18. Parvatiyar, M. S., J. R. Pinto, …, J. D. Potter. 2010. Predicting cardiomyopathic phenotypes by altering Ca^{2+} affinity of cardiac troponin C. *J. Biol. Chem.* 285:27785–27797.

19. Tikunova, S. B., and J. P. Davis. 2004. Designing calcium-sensitizing mutations in the regulatory domain of cardiac troponin C. *J. Biol. Chem.* 279:35341–35352.

20. Ryckaert, J.-P., G. Ciccotti, and H. J. C. Berendsen. 1977. Numerical integration of the cartesian equations of motion of a system with constraints: molecular dynamics of *n*-alkanes. *J. Comput. Phys.* 23: 327–341.

21. Wang, X., M. X. Li, and B. D. Sykes. 2002. Structure of the regulatory N-domain of human cardiac troponin C in complex with human cardiac troponin I147–163 and bepridil. *J. Biol. Chem.* 277:31124–31133.

22. Amaro, R. E., R. Baron, and J. A. McCammon. 2008. An improved relaxed complex scheme for receptor flexibility in computer-aided drug design. *J. Comput. Aided Mol. Des.* 22:693–705.